



# High-dimensional counterdiabatic quantum computing

Diego Tancara <sup>1</sup> and Francisco Albarrán-Arriagada <sup>2</sup>

<sup>1</sup>*Departamento de Física, Universidad de Santiago de Chile (USACH), Avenida Víctor Jara 3493, 9170124, Santiago, Chile.*

<sup>2</sup>*Departamento de Física, CEDENNA, Universidad de Santiago de Chile (USACH),*

*Avenida Víctor Jara 3493, 9170124, Santiago, Chile.\**

(Dated: October 15, 2024)

The digital version of adiabatic quantum computing enhanced by counterdiabatic driving, known as digitized counterdiabatic quantum computing, has emerged as a paradigm that opens the door to fast and low-depth algorithms. In this work, we explore the extension of this paradigm to high-dimensional systems. Specifically, we consider qutrits in the context of quadratic problems, obtaining the qutrit Hamiltonian codifications and the counterdiabatic drivings. Our findings show that the use of qutrits can improve the quality of the solution up to 90 times compared to qubits counterpart. We test our proposal on 1000 random instances of the multi-way number partitioning, max 3-cut, and portfolio optimization problems, demonstrating that, in general, without prior knowledge, it is always better to use high-dimensional systems instead of qubits. Finally, considering the state-of-the-art in quantum platforms, we show the experimental feasibility of our high-dimensional counterdiabatic quantum algorithms at least in a full digital form. This work paves the way for the efficient codification of optimization problems in high-dimensional spaces and their efficient implementation using counterdiabatic quantum computing.

## INTRODUCTION

Quantum computing has received significant attention in recent years. The emergence of quantum technology start-ups and increased funding from government agencies have led to unprecedented investment in the field. This surge is driven by the potential of quantum technologies to surpass the classical limits of traditional devices. Several experiments in quantum computing have claimed quantum advantage [1–5], that is, a computational problem where a quantum computer outperforms its classical counterpart. This breakthrough opens the door to solving previously intractable problems with potential industrial applications.

Some notable areas of quantum computing application include quantum simulation, machine learning, and optimization problems [6–8], where the paradigm of digital gate-based quantum computing take advantage due to its universality [9, 10] and experimental implementations in different platforms [11–13]. However, the current noisy intermediate-scale quantum (NISQ) devices present limitations, necessitating algorithmic improvements to achieve quantum advantage for industrial purposes [14, 15].

Another interesting paradigm for quantum computing is the adiabatic quantum computing (AQC), which provides promising algorithm to solve optimization problems [16]. AQC involves an adiabatic evolution from a Hamiltonian with an easily generated ground state to a final Hamiltonian encoding the solution to the optimization problem. According to the quantum adiabatic theorem, the time-dependent state follows the instantaneous ground state during the adiabatic evolution. While AQC provides a standardized form to encode optimization problems in a Hamiltonian, its implementation is hampered by the long coherence times required for adiabatic evolution. One possible implementation of AQC can be done by the digitalization of the adiabatic evolution [17]. Nevertheless, due to the long evolution time required by adiabatic

evolutions, the digitalization request long circuit depth, which translate in low fidelity and impractical for NISQ devices. It is important to mention, that the scalability of the total time of adiabatic evolution in AQC is equivalent to the scalability of the circuit depth for standard quantum computing algorithms [18, 19].

To reduce the time of adiabatic protocols, shortcut to adiabaticity (STA) techniques emerge to accelerate these processes [20], specifically the counterdiabatic (CD) driving has yielded promising results [21–23]. However the exact calculation of counterdiabatic fields are in general a complex task since it request the knowledge of the energy spectrum during all the evolution, being impractical. In this line, approximate expressions for the CD terms open the door for implementables CD protocols [24–28]. In this context, digitized counterdiabatic quantum algorithms (DCQA) have been recently proposed to enhance quantum algorithms on NISQ devices [29]. This approach has been tested in various areas, including the enhanced quantum approximate optimization algorithm (QAOA) [30, 31], as well as in factorization, biology, and finance problems [32–34].

Another possible enhancement for quantum computing is the use of high-dimensional quantum systems, called qudits [35]. The principal enhancement in the use of qudits, is the amount of information stored compared to qubits, reducing the complexity of a quantum algorithm [36] allowing more efficient codifications. This potential has led to the exploration of different physical platforms for the use of qudits, in this line, the generation of entangled qudits states has been theoretically proposed and experimentally implemented [37–39].

In addition to these developments, quantum gates for high-dimensional quantum computing have been demonstrated across multiple platforms. For instance, single photons have been used to implement X-qudit gates [40], as well as, superconducting circuits and trapped ions have demonstrated the implementation of quantum gates for three-level (qutrits) and

five-level systems [41–43]. In this work, we study the application of the CD protocol for qutrits to address optimization problems and enhance algorithm performance compared to qubits. Specifically, we focus on the codification and performance of multi-way number partitioning, max 3-cut, and portfolio optimization problems.

## METHODS

As we are focused in an adiabatic evolution enhanced by counterdiabatic drivings for high dimensional systems, specifically for qutrits. In this section we describe the framework to obtain the initial and final Hamiltonian for different problems, we briefly introduce the nested commutator approach to get an approximation for the counterdiabatic driving. Finally we show how the different terms can be implemented by digitalization considering the current state-of-the-art.

### Hamiltonian codification

We consider an evolution governed by a time-dependent Hamiltonian

$$H(t/T) = [1 - \lambda(t/T)]H_I + \lambda(t/T)H_F, \quad (1)$$

where  $H_I$  is the initial Hamiltonian,  $H_F$  the final Hamiltonian,  $T$  the total evolution time and  $\lambda$  the schedule function. In general,  $H_I$  consider only local terms, which ground state is a uniform superposition of all the states. In the qubit case  $H_I = -\sum_j \sigma_j^x$ . Following the same structure we define the next initial Hamiltonian

$$H_I = -\omega_0 \sum_j X_j, \quad (2)$$

where the subindex  $j$  refers to the  $j$ th qutrit and the matrix  $X$  is given by

$$X = \begin{pmatrix} 1 & 1 & 0 \\ 1 & 0 & 1 \\ 0 & 1 & 1 \end{pmatrix}, \quad (3)$$

the ground state  $|\phi_g\rangle$  of  $H_I$  is given by

$$|\phi_g\rangle = \bigotimes_j |+\rangle_j; \quad |+\rangle_j = \sqrt{\frac{1}{3}}(|0\rangle_j + |1\rangle_j + |2\rangle_j), \quad (4)$$

that is, the flat superposition of all the possible states in the computational basis for qutrits.

As we consider classical optimization problems, the final Hamiltonian has the form

$$H_F = \sum_j \omega_j^{(1)} Z_j + \sum_{j,k} \omega_{j,k}^{(2)} Z_j Z_k + \sum_{j,k,l} \omega_{j,k,l}^{(3)} Z_j Z_k Z_l + \dots, \quad (5)$$

where we can consider all the  $p$ -local terms with

$$Z = \begin{pmatrix} 1 & 0 & 0 \\ 0 & 0 & 0 \\ 0 & 0 & -1 \end{pmatrix}. \quad (6)$$

In this work we consider three paradigmatic examples, the multi-way number partitioning problem, max k-cut problem and the portfolio optimization problem.

### Multi-way number partitioning problem

This problem consider a set  $S$  of  $N$  numbers into different partitions. The goal is that the sum of the elements of each partition be as equal as possible to the others. We will consider the specific case of three partitions, then we use qutrits to codify it. The set  $S$  is defined as

$$S = \{s_1, s_2, \dots, s_N\}, \quad (7)$$

where  $s_j$  is a real number. As usual, we consider three different labels, one for each partition. Each label is a value of a trinary variable, then we consider as much trinary variables as numbers in the set  $S$ . Specifically we use the trinary variable  $q_j = \{1, 0, -1\}$ , where  $q_j = 1$  is  $s_j$  belongs the first partition,  $q_j = 0$  is  $s_j$  is in the second partition and  $q_j = -1$  if  $s_j$  is an element of the third partition. Now, we define  $C_k$  the sum of the elements in the partition  $k$ , then we have that:

$$C_1 = \sum_{j=1}^N \frac{1}{2} q_j (q_j + 1) s_j \quad (8)$$

$$C_2 = \sum_{j=1}^N (1 - q_j)(1 + q_j) s_j \quad (9)$$

$$C_3 = \sum_{j=1}^N \frac{1}{2} q_j (q_j - 1) s_j. \quad (10)$$

As in this case the goal is that  $C_1$ ,  $C_2$  and  $C_3$  be as equal as possible, the minimization is over the function

$$F = (C_1 - C_2)^2 + (C_1 - C_3)^2. \quad (11)$$

We note that by transitivity the term  $(C_2 - C_3)$  can be neglected. Changing the trinary variables  $q_j$  to qutrits operators  $Z_j$  we obtain the next Hamiltonian

$$\begin{aligned} H_F &= \frac{1}{4} \left[ \sum_j (3G_j - Z_j - 2) s_j \right]^2 + \left[ \sum_j Z_j s_j \right]^2 \\ &= \frac{1}{4} \sum_{j,k} (9G_j G_k - 6G_j Z_k - 12G_j \\ &\quad + 4Z_j + 5Z_j Z_k + 4) s_j s_k, \end{aligned} \quad (12)$$

where  $G_j = Z_j^2$  is a one body operator of the form

$$G_j = \begin{pmatrix} 1 & 0 & 0 \\ 0 & 0 & 0 \\ 0 & 0 & 1 \end{pmatrix}. \quad (13)$$

Therefore, the Hamiltonian (44) has only one and two body operators, that is a quadratic form.

#### Max $k$ -cut

In this problem we consider a graph  $\mathcal{G}(V, E)$  composed of  $V$  vertices and  $E$  edges. The idea is to classify the vertices in  $k$  different groups in order to maximize the edges shared between the groups. We consider the max 3-cut problem, that means that we consider three partitions. Similar to the previous case, we use a trinary variable for each vertex to indicate which partition it belongs to. As each variable  $q_j$  represent the label of the vertex  $v_j$ , we need to minimize the case when two vertices comes from different paritions. If we consider the product  $q_j q_k$ , it is 1 if  $q_j = q_k$  (except for  $q_j = 0$ ), and 0 and  $-1$  in other case. It means that the minimal value of the term  $q_j q_k (q_j q_k + 1)$  is obtained for  $q_j \neq q_k$  (except for  $q_j = q_k = 0$ ).

Therefore, our minimization function is the sumation of the above term for the vertices  $j$  and  $k$  that share an edge, and for the case  $q_j = q_k = 0$  we add a penalization term obtaining

$$F = \sum_{(j,k) \in E} \left[ q_j q_k (q_j q_k + 1) + \alpha (1 - q_j^2)(1 - q_k^2) \right], \quad (14)$$

where  $\alpha$  is the penalty constant. Transforming the trinary variable to qutrit operators we obtain the following Hamiltonian for max 3-cut:

$$\begin{aligned} H_F &= \sum_{(j,k) \in E} \left[ Z_j Z_k (Z_j Z_k + 1) + \alpha (1 - Z_j^2)(1 - Z_k^2) \right] \\ &= \sum_{(j,k) \in E} \left[ (1 + \alpha) G_j G_k + Z_j Z_k - \alpha (G_j + G_k) \right], \quad (15) \end{aligned}$$

where we have obtained a quadratic Hamiltonian as in the previous case.

#### Portfolio Optimization

The last example that we consider is the Markowitz portfolio optimization [44]. The goal here is to distribute a budget  $b$  across  $n$  assets to maximize expected returns while minimizing risk. To estimate the expected return, we consider the historical market return data, while the risk is quantified using the covariance matrix of the historical data. The cost function for this problem is given by:

$$F = \theta_1 \sum_{j=1}^n m_j p_j + \theta_2 \sum_{j,j'=1}^n \rho_{j,k} p_j p_{j'} + \theta_3 \left( \sum_{j=1}^n G_j b p_j - b \right)^2, \quad (16)$$

where  $m_j$  is the expected return of asset  $j$ ,  $\rho_{j,k}$  is the covariance matrix element that show the variance of the  $k$ th asset with the  $j$ th asset, and  $p_j$  is an integer related to the portion of the  $j$ th asset in the portfolio.  $G_f$  is the granularity function such that

$\sum_j G_f p_j = 1$ , that is a normalization constant. For example, if we consider  $g$  trinary digits per assets  $G_f = 1/(3^g - 1)$ . Additionally,  $\theta_1, \theta_2, \theta_3$  are the Lagrange multipliers, ponderate the expected returns, risk, and constrain of budget respectively.

In a trinary representation we gave

$$p_j = \sum_{k=1}^g 3^{k-1} q_{u_{j,k}}, \quad (17)$$

where the index  $u_{j,k} = (j-1)g+k$ , and  $q_j \in \{0, 1, 2\}$ , the index  $j$  is the label for the asset and  $k$  the term in the sumatory. From now on, we will refer to  $u_{j,k}$  as  $u$ . As we consider  $g$  trinary digits per asset, then for the total problem we need to consider  $ng$  trinary digits.

To obtain the Hamiltonian, we replace the trinary variables by

$$q_u \rightarrow Q_u = Z_u + I, \quad (18)$$

in the cost function, where  $I$  is the identity for qutrits and  $Q_u$  is one body operator of the form:

$$Q_u = \begin{pmatrix} 2 & 0 & 0 \\ 0 & 1 & 0 \\ 0 & 0 & 0 \end{pmatrix}. \quad (19)$$

Therefore, in terms of  $Q_u$ , the Hamiltonian have the following form

$$\begin{aligned} H_F &= \theta_1 \sum_{j=1}^n m_j \sum_{k=1}^g 3^{k-1} Q_u \\ &+ \theta_2 \sum_{j,j'=1}^n \rho_{j,j'} \sum_{k,k'=1}^g 3^{k-1} Q_u 3^{k'-1} Q_{u'} \\ &+ \theta_3 \left( \sum_{j=1}^n G_j b \sum_{k=1}^g 3^{k-1} Q_u - b \right)^2 \\ &= \sum_{j=1}^n \sum_{k=1}^g \alpha_{jk} Q_u + \sum_{j,j'=1}^n \sum_{k,k'=1}^g \beta_{jj'}^{kk'} Q_u Q_{u'} + \theta_3 b^2, \quad (20) \end{aligned}$$

where:

$$\begin{aligned} \alpha_{jk} &= 3^{k-1} (\theta_1 m_j - \theta_3 2b^2 G_f), \\ \beta_{jj'}^{kk'} &= 3^{k+k'-2} (\theta_2 \rho_{jj'} + \theta_3 G_f^2 b^2) \end{aligned} \quad (21)$$

#### Counterdiabatic drivings

To accelerate adiabatic protocols, we can use counterdiabatic drivings, that is, a control field to suppress the unwanted transitions between instantaneous eigenstates. The time-dependent Hamiltonian modified by the addition of the CD term reads

$$H(t) = \underbrace{(1 - \lambda) H_1 + \lambda H_F}_{H_{\text{ad}}} + \lambda A_\lambda, \quad (22)$$

where  $A_\lambda$  is called the adiabatic gauge potential (AGP), and the time dependence is given in the schedule function  $\lambda$ . The AGP satisfy

$$[i\partial_\lambda H_{\text{ad}} - [A_\lambda, H_{\text{ad}}], \hat{H}_{\text{ad}}] = 0. \quad (23)$$

The exact form of  $A_\lambda$  is determined by the instantaneous eigenstates of  $H_{\text{ad}}$ , being impractical to calculate [23]. Nevertheless, there are approximations to the ADG such that:

$$A_\lambda^l = i \sum_{k=1}^l \alpha_k O_{2k-1}, \quad (24)$$

with

$$O_k = \underbrace{[H_{\text{ad}}, [H_{\text{ad}}, \dots [H_{\text{ad}}, \partial_\lambda H_{\text{ad}}]]]}_k. \quad (25)$$

The coefficients  $\alpha_k$  satisfy the next linear system of equations [45]:

$$\begin{pmatrix} \Gamma_2 & \Gamma_3 & \cdots & \Gamma_{l+1} \\ \Gamma_3 & \Gamma_4 & \cdots & \Gamma_{l+2} \\ \vdots & \vdots & \ddots & \vdots \\ \Gamma_{l+1} & \Gamma_{l+2} & \cdots & \Gamma_{2l} \end{pmatrix} \begin{pmatrix} \alpha_1 \\ \alpha_2 \\ \vdots \\ \alpha_l \end{pmatrix} = - \begin{pmatrix} \Gamma_1 \\ \Gamma_2 \\ \vdots \\ \Gamma_l \end{pmatrix}, \quad (26)$$

where  $\Gamma_k = \|\hat{O}_k\|_F^2$  is the squared Frobenius norm of the nested commutator. For  $l = 1$  we have

$$\alpha_1 = -\frac{\Gamma_1}{\Gamma_2}. \quad (27)$$

In this work, we will focus in  $l = 1$ , then we consider the next approximation for the AGP

$$A_\lambda \approx i \frac{\Gamma_1}{\Gamma_2} [H_{\text{ad}}, \partial_\lambda H_{\text{ad}}] = i \frac{\Gamma_1}{\Gamma_2} [H_I, H_F] \quad (28)$$

## RESULTS

To show the performance of our solution we will consider how much our solution minimize the energy of the final Hamiltonian. For this propose we use the a metric defined by the percental error of the energy at the end of the evolution given by

$$\mathcal{R} = \frac{E(T) - E_g}{\Delta E}, \quad (29)$$

where  $E(t) = \langle \psi(t) | H(t/T) | \psi(t) \rangle$  is the mean instantaneous energy, and  $E_g$  is the ground state energy of  $H_F$ .  $\Delta E$  is the gap between the two different minimal energies of  $H_F$ .  $\mathcal{R}$  said us how good is the our solution related to the energy gap  $\Delta E$ . Also we consider three different regimes, that is, for short time or impulse regime, medium time and adiabatic or large time regime. First, we consider specific cases as example of the

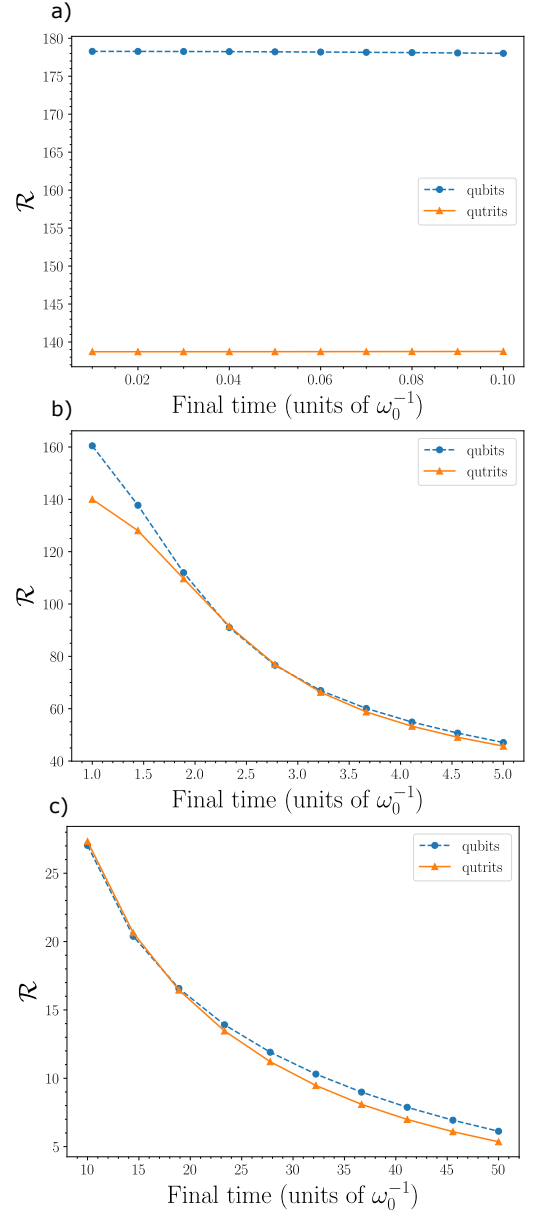


FIG. 1. Three partition multi-way number partitioning problem for the set  $\{0.8, 1.1, 1.1, 0.7, 1, 0.3\}$  for different regimes, that is, a: short final time or impulse regime, b: medium final time, and c: long final time or adiabatic regime.

performance of our high-dimensional counterdiabatic quantum computing (HDCQC) protocol compared to the standard qubit paradigm.

Figure 1 shows the  $\mathcal{R}$  metric for the multiway number partitioning problem, where we consider the set  $\{0.8, 1.1, 1.1, 0.7, 1, 0.3\}$ . We observe a small advantage in the use of qutrits over qubits, which can be appreciated only in the impulse regime. We note that in Fig 1 a, the value of  $\mathcal{R}$  is high for both, qutrit and qubits, which implies that even if we have a better performance for the qutrit case, it is far from the solution.

For the max 3-cut problem, Fig. 2 shows the  $\mathcal{R}$  metric for a six nodes wheel graph ( $W_6$ ). We can observe that in these case the performance of qutrits is appreciable even in the middle time regime as can be seen in Fig. 2 a and b. Also, the values for  $\mathcal{R}$  goes below 1 in all the regimes which indicate that our solutions are close to the ground state even for the impulse regime.

Now, Fig. 3 shows the performance using qutrits and qubits for the portfolio optimization problem. As an example we consider the real data provided by yfinance [48] for the assets: Apple, Microsoft, Google, Amazon, Tesla and Netflix

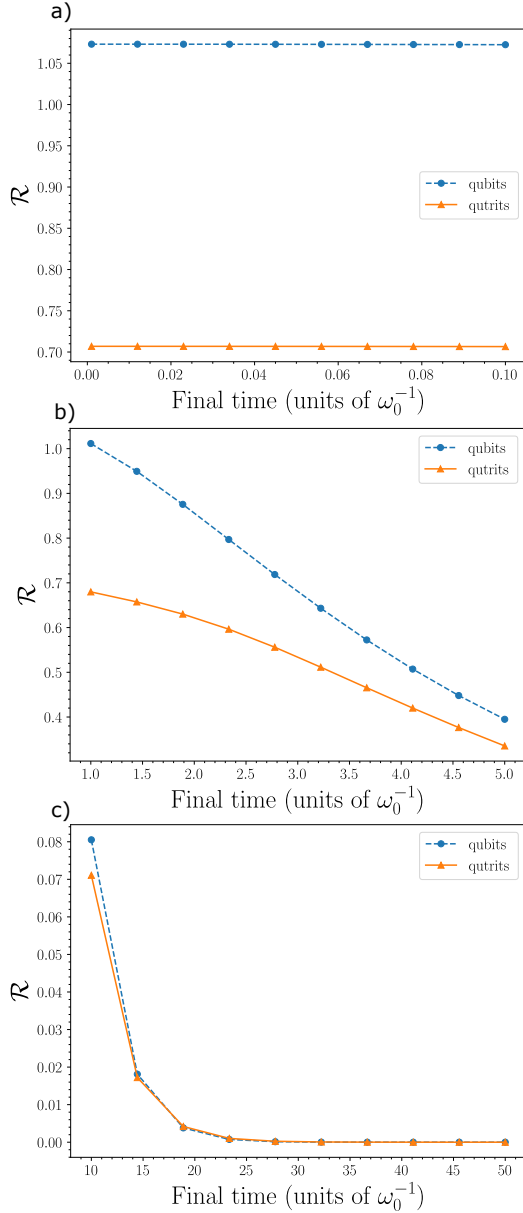


FIG. 2. Max k-cut for connectivity of wheels  $W_6$  (6 nodes), for different regimes, that is, a: short final time or impulse regime, b: medium final time, and c: long final time or adiabatic regime.

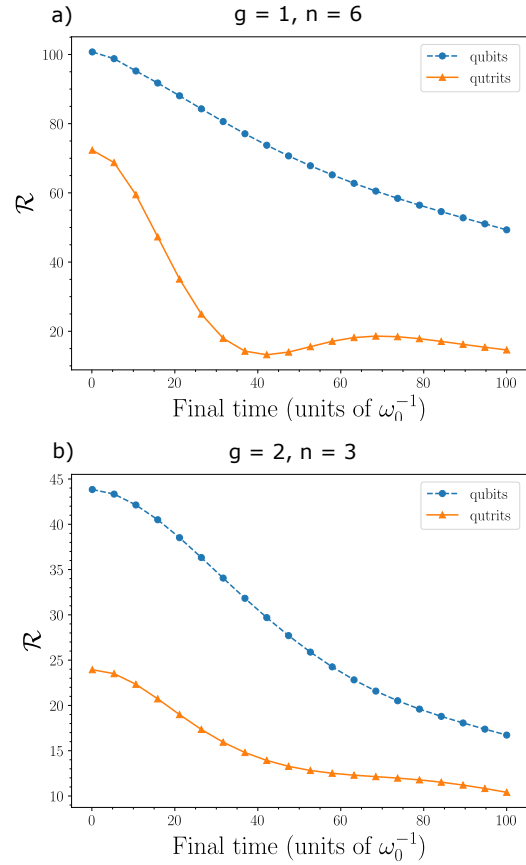


FIG. 3. Portfolio optimization, comparison between qubits and qutrits for a:  $g = 1, n = 6$  and b:  $g = 2, n = 3$ .

for the time period 2020-2023. Using this data the mean expected returns and covariance matrix are

$$m = 10^{-4}(10.24, 1.411, 5.730, 8.082, 4.122, 29.64)$$

$$\rho = 10^{-4} \begin{pmatrix} 5.413 & 3.799 & 3.696 & 4.133 & 3.690 & 5.495 \\ 3.799 & 6.062 & 3.638 & 3.781 & 4.768 & 5.343 \\ 3.696 & 3.638 & 4.730 & 3.953 & 3.543 & 4.474 \\ 4.133 & 3.781 & 3.953 & 4.794 & 3.631 & 4.987 \\ 3.690 & 4.77 & 3.543 & 3.631 & 1.067 & 6.067 \\ 5.495 & 5.343 & 4.474 & 4.987 & 6.067 & 20.67 \end{pmatrix} \quad (30)$$

For Fig. 3 a, we consider the mentioned six assets observing that the improvement of qutrits over qubits is appreciable over all the evolution. In the mentioned figure we use  $g = 1$ , which means that  $G_f = 1/2$ . Next in Fig. 3 b, we consider only three first asset of the above list, but using  $g=2$ , which means that  $G_f = 1/8$ . We can see in this figure that again the performance of qutrits over qubits is appreciable better for the range  $T \in [0, 100]$ , nevertheless in all the cases  $\mathcal{R} > 10$ , which suggest that even for  $T = 100\omega_0^{-1}$  we are not reaching the adiabatic regime.

In order to understand the enhancement produced by the use of qutrits instead of qubits, we define the success probability using  $j$ -dimensional systems as:

$$P_j(T) = \sum_{g=1}^{d_j} |\langle g_j | \psi_j(T) \rangle|^2, \quad (31)$$

where are  $d$  degenerate groundstates, and  $j$  is the dimension of the qudits used in the computational proces, that is  $j = 2$  for qubits and  $j = 3$  for qutrits. The time  $T$  represent the total time of the evolution, then  $\lim_{T \rightarrow \infty} P_j(T) = 1$ . To obtain a metric for the enhancement, we can define the success probability enhancement for a time  $T$  as:

$$\mathcal{P}_{j/k}(T) = \frac{P_j(T)}{P_k(T)}, \quad (32)$$

in our case we will focus in  $\mathcal{P}_{3/2}(T)$ , that is the comparison between qutrits and qubits. Also, we need to remind that we are considering evolutions with CD term given by the approximation for the AGP in Eq. (28). To obtain representative results we consider the success probability enhancement for 1000 random instances for each problem decribed in the previous section, and again for different total time  $T = 0.1\omega_0^{-1}$ ,  $T = \omega_0^{-1}$  and  $T = 10\omega_0^{-1}$ .

Figure 4 a shows the results of  $\mathcal{P}_{3/2}(T)$  for the multi-way number partitioning problem for a set of six random numbers in the range  $[0, 1]$ , where we can see that larger enhancement can be reached for short time  $T$  as we can expect. In this case we can observe that there are instancer for which  $\mathcal{P}_{3/2}(T) < 1$ , that is that the use of qutrits do not provide a benefit, but in the most cases the obtain  $\mathcal{P}_{3/2}(T) > 1$ .

Figure 4 b shows the results of  $\mathcal{P}_{3/2}(T)$  for the max 3-cut problem for random graphs of six nodes, where we can see that larger enhancement can be reached for short time  $T$  as we can expect. In this case we can observe that for all the 1000 random instances  $\mathcal{P}_{3/2}(T) > 1$ , which suggest that for this problem always is better the use of qutrits instead of qubits. Also, it is necessary to remarck that therar instances where  $\mathcal{P}_{3/2}(T) > 90$  which indicates that the use of the qutrits can enhance the solution around two order of magnitudes.

## ANALISYS

It is interesting to note that according to our results, there are cases where the use of qutrits is not better to qubits even if the codification of the problem is more natural for qutrits. Nevertheless, if the consider the mean success probability enhancement ( $\bar{\mathcal{P}}_{3/2}$ ) we can note in the cases under study always is larger than 1. For example for the multi-way number partitioning problem we have  $\bar{\mathcal{P}}_{3/2}(0.1\omega_0^{-1}) = 1.31$ ,  $\bar{\mathcal{P}}_{3/2}(\omega_0^{-1}) = 1.23$  and  $\bar{\mathcal{P}}_{3/2}(10\omega_0^{-1}) = 1.07$ , and the percentage of instances with enhancement larger than 1 are 84.6%, 79.8% and 74.8% for the same times respectively. It suggest that without previous knowledge, it is a good idea to codify and use qutrits instead of qubits.

On the other hand, for max 3-cut problem in all the cases we obtain enhancement, where the mean success probability

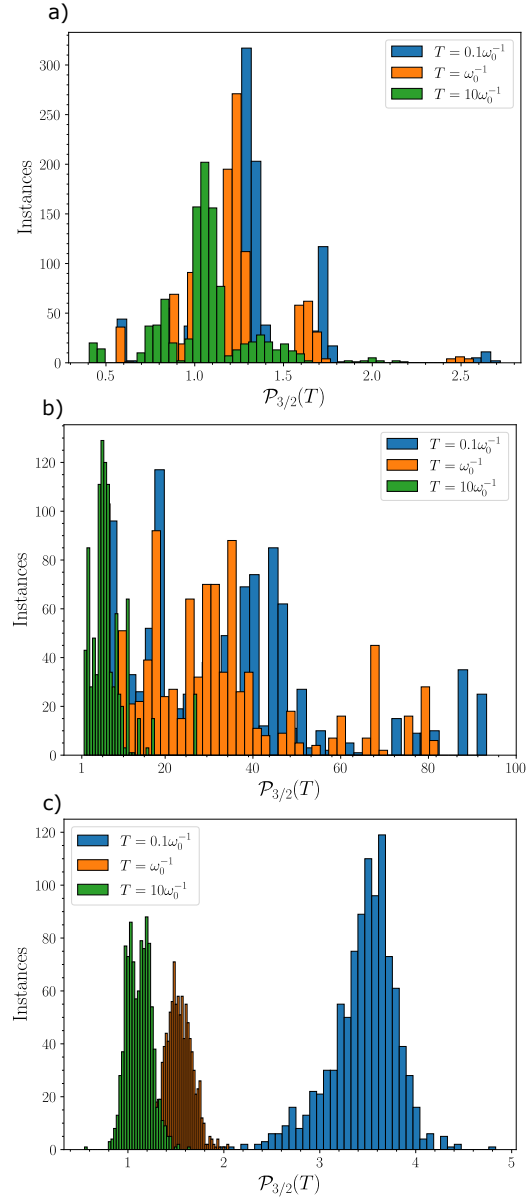


FIG. 4. Success probability enhancement for 1000 random instances for a: multi-way number partitioning for six random numbers in range  $[0, 1]$ , b: Max 3-cut for six nodes graphs with random connectivity, and c: Portfolio optimization for 6 assets with random expected return and covariance matrix.

enhancement are  $\bar{\mathcal{P}}_{3/2}(0.1\omega_0) = 35.34$ ,  $\bar{\mathcal{P}}_{3/2}(\omega_0) = 30.41$  and  $\bar{\mathcal{P}}_{3/2}(10\omega_0) = 6.99$ , which indicates that an efficient codification in high dimensional systems always is better for max 3-cut problem.

For the portfolio optimization problem we have that for  $T = 0.1\omega_0^{-1}$  and  $T = 1\omega_0^{-1}$  all the cases get enhancement, where the mean success probability enhancement are  $\bar{\mathcal{P}}_{3/2}(0.1\omega_0) = 3.56$  and  $\bar{\mathcal{P}}_{3/2}(\omega_0) = 1.54$ . For  $T = 10\omega_0^{-1}$  we have that the percentage of instances with enhancement surpass 80% with a mean enhancement  $\bar{\mathcal{P}}_{3/2}(10\omega_0) = 1.12$ , which indicates that



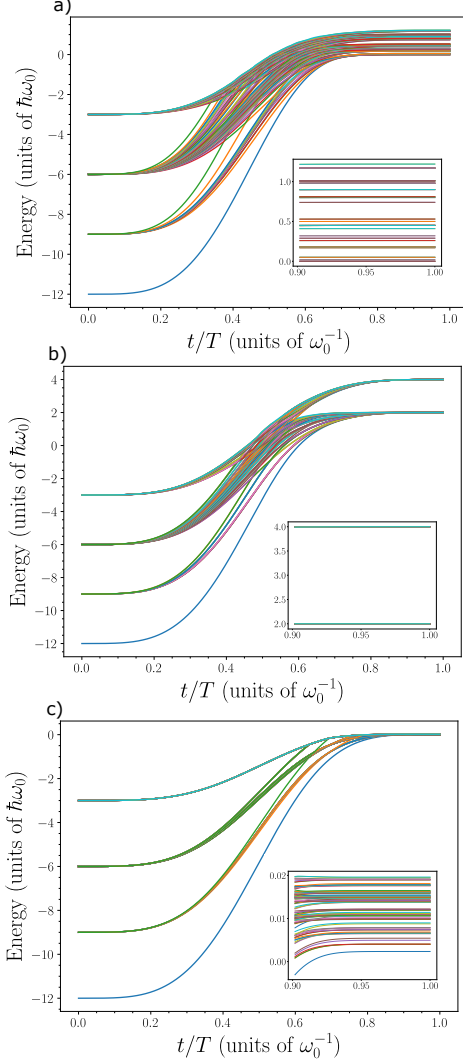


FIG. 5. Spectrum for adiabatic Hamiltonian  $H(t)$  of 100 first levels vs normalized time for qutrits formulation. a: Multiway number partitioning with the set of numbers is  $\{8/10, 11/10, 15/10, 7/10, 10/10, 3/10\}$ . b: Max 3-cut with the connectivity  $W_6$ . c: Portfolio optimization with  $g = 1$  and 6 assets ('AAPL', 'MSFT', 'GOOGL', 'AMZN', 'TSLA', 'NFLX').

an efficient codification in high dimensional systems provides in general enhancement for protafolio optimization, less than in the max 3-cut problem but more that in the multiway number partitioning problem.

In order to understand why there are cases with  $\mathcal{P}_{3/2} < 1$  and cases with  $\mathcal{P}_{3/2} \sim 100$ , we plot the energy spectrum during a time-evolution in Fig. 5 to see the behaviour of it for different cases. We can observe that in our best case, that is the max 3-cut problem (panel b), the energies of the possible solutions (degenerate ground state), are far from the next energy, obtaining few level crossings. Now, even if, for the portfolio optimization problem (panel c) the final energy gap is smaller than in the number partitioning problem (panel a), we have

more level crossings in the last one, which favoring the unwanted energy transitions. It means that the performance of our HDQCQ is strictly related with the level crossing during the evolution, as is suggesting by the quantum adiabatic theorem.

### Physical implementation

One possible implementation of high-dimensional counterdiabatic quantum computing (HDCQC) is by digitalization of the adiabatic evolution enhanced with counterdiabatic drivings as in proposed for qubits in ref [29], and then implement it in a quantum platform that allows universal quantum computing with qutrits.

The basic idea is to write the time evolution governed by the Hamiltonian (22) as

$$\begin{aligned}
 U(t) &= \mathcal{T} e^{-\frac{i}{\hbar} \int_0^t \{[1-\lambda(\tau)]H_1 + \lambda(\tau)H_F + \dot{\lambda}(\tau)A_\lambda(\tau)\} d\tau} \\
 &\approx e^{-\frac{i}{\hbar} \sum_j \{[1-\lambda(j\Delta t)]H_1 + \lambda(j\Delta t)H_F + \dot{\lambda}(j\Delta t)A_\lambda(j\Delta t)\} \Delta t} \\
 &\approx \prod_j e^{-\frac{i}{\hbar} \{[1-\lambda(j\Delta t)]H_1 + \lambda(j\Delta t)H_F + \dot{\lambda}(j\Delta t)A_\lambda(j\Delta t)\} \Delta t} \\
 &\approx \prod_j e^{-\frac{i}{\hbar} [1-\lambda(t_j)]H_1 \Delta t} e^{-\frac{i}{\hbar} \lambda(t_j)H_F \Delta t} e^{-\frac{i}{\hbar} \dot{\lambda}(t_j)A_\lambda(t_j) \Delta t}, \quad (33)
 \end{aligned}$$

where  $t_j = t_{j-1} + \Delta t = j\Delta t$ . If  $\Delta t$  is small enough this approximation reproduce the adiabatic evolution enhanced by counterdiabatic drivings.

Now, the implementation of an arbitrary unitary transformation in high-dimensional systems, can be done by the suitable combination of all two-level rotations of the high-dimensional system plus a two-body controlled phase gate. Such set of transformations have been reported in different physical platforms, where superconducting circuits and trapped ions are promising for universal qutrit quantum computing. For example in Ref. [46] a two-level qutrit rotation has been proposed using Zeeman's level structure in trapped ions, where they consider a model with dipole and rotating wave approximations and five levels  $i = 0, 1, 2, 3, 4$ , with two of them (3, 4) are adiabatically eliminated. For this case considering only carrier transitions and detuning conditions, we obtain the following evolution operator:

$$U_{\phi, k, k'} = \begin{pmatrix} 1 + |g(k)|^2 C(\phi) & g(k)g^*(k')C(\phi) & -ig(k)\sin(\phi) \\ g(k')g^*(k)C(\phi) & 1 + |g(k)|^2 C(\phi) & -ig(k)\sin(\phi) \\ -ig^*(k)\sin(\phi) & -ig^*(k')\sin(\phi) & \cos(\phi) \end{pmatrix} \quad (34)$$

where  $\phi = \Omega t$ ,  $\Omega = |k|^2 + |k'|^2$  with  $k = \Omega_{40}\Omega_{42}^*/\Delta$  and  $k' = \Omega_{30}\Omega_{31}^*/\Delta$  where  $\Omega_{i,j}$  are coupling between level  $i$  and  $j$ ,  $g(k) = k/\Omega$  and  $C(\phi) = \cos(\phi) - 1$ . By setting  $\phi$ ,  $k$  and  $k'$  in Eq. (34) we can implement any qutrit rotation, for example two-level transformations of the form [46]:

$$\begin{aligned}
 U_{ij} &= \cos(\alpha_{ij})|i\rangle\langle i| + |j\rangle\langle j| \\
 &- e^{i\beta_{ij}} \sin(\alpha_{ij})|i\rangle\langle j| - e^{-i\beta_{ij}} \sin(\alpha_{ij})|j\rangle\langle i|, \quad (35)
 \end{aligned}$$

can be obtained by fixing

$$\cos(\alpha_{ij}) = \begin{cases} \frac{|k|^2 - |k'|^2}{|k|^2 + |k'|^2} & \text{if } i = 1, j = 2 \\ \cos(|k|t) & \text{if } i = 0, j = 2, \\ \cos(|k'|t) & \text{if } i = 0, j = 1 \end{cases} \quad (36)$$

$$e^{i\beta} = \begin{cases} \frac{|k|^2 - |k'|^2}{|k|^2 + |k'|^2} & \text{if } i = 1, j = 2 \\ \cos(|k|t) & \text{if } i = 0, j = 2, \\ \cos(|k'|t) & \text{if } i = 0, j = 1 \end{cases} \quad (37)$$

allowing us the implementation of all the local evolutions.

Now, the implementation of the bilocal terms such as  $e^{i\alpha Z_i Z_j}$ ,  $e^{i\alpha Z_i G_j}$  and  $e^{i\alpha Z_i Y_j}$ , where the last one correspond to an interaction term in counterdiabatic approximation, where

$$Y_j = \begin{pmatrix} 0 & -i & 0 \\ i & 0 & -i \\ 0 & i & 0 \end{pmatrix}, \quad (38)$$

can be done by using a controlled phase gate. In the case of trapped ions it can be done through the center-of-mass motion, which is controlled by tuning a Raman transition to a specific red sideband as is shown in Ref. [46]. With a effective Hamiltonian they model a center-mass phonons by annihilation and creation operators, coupled to electronic transition  $|0\rangle \rightarrow |q\rangle$ , with  $q = 1, 2$ . In particular we can obtain an effective unitary transformation between the qutrit  $m$  and the center of mass of the form

$$\begin{aligned} U_m^{l,q}(\varphi)|0\rangle_m|0\rangle &= |0\rangle_m|0\rangle \\ U_m^{l,q}(\varphi)|0\rangle_m|1\rangle &= \cos\left(\frac{l\pi}{2}\right)|0\rangle_m|1\rangle - ie^{-i\varphi} \sin\left(\frac{l\pi}{2}\right)|q\rangle_m|0\rangle \\ U_m^{l,q}(\varphi)|q\rangle_m|0\rangle &= \cos\left(\frac{l\pi}{2}\right)|q\rangle_m|0\rangle - ie^{i\varphi} \sin\left(\frac{l\pi}{2}\right)|0\rangle_m|1\rangle \end{aligned} \quad (39)$$

where  $l\pi/2 = \Omega_q \eta t/2$ , with  $\Omega_q$  is the effective Rabi frequency of transition  $|0\rangle \rightarrow |q\rangle$  after adiabatic elimination of upper excited levels,  $\eta$  is the Lamb-Dicke parameter and  $\varphi$  is the laser phase. This interaction allow us to produce any controlled-phase gate trough the center of mass, obtaining the basic key ingredients for universal qutrit quantum computing [36], and therefore an experimentally feasible way to implement our HDCQC paradigm.

## CONCLUSION

In the present work, we study the use of high-dimensional systems (qutrits) for quantum computing in the counterdiabatic quantum computing paradigm. Specifically we study the performance of a qutrit codification for the multi-way number partitioning, max 3-cut and portfolio optimization problem. We find that in general the use of qutrits provides better results than the qubits counterpart, where in some cases the enhancement factor reach 90, that is, almost two magnitud orders,

where the enhancement is related to the density of level crossing during the evolution, being the case with more enhancement the max 3-cut problem, with a mean enhancement of the 35.34, 30.41 and 6.99 for final time  $T = \{0.1\omega_0^{-1}, \omega_0^{-1}, 10\omega_0^{-1}\}$ , even if, for the worst cases, that is number partitioning problem we have that the mean enhancement are 1.31, 1.23 and 1.07 for the same final times, siggesting that always is better use a high-dimensional codification.

Finally, we analyse the curret state-of-the-art in trapped ionnes which allows the experimental implementation of universal qutrit quantum computing, allowing the implementation of the digital version of our high-dimensional counterdiabatic quantum computing proposal. This work provide numerical evidence of the benefit in the use of high dimensional systems, and shows its fesiability according to the current state-of-the-art, paving the way to a more efficient quantum computing algorithms.

## ACKNOWLEDGMENTS

We acknowledge financial support from Agencia Nacional de Investigación y Desarrollo (ANID): Financiamiento Basal para Centros Científicos y Tecnológicos de Excelencia grant No. AFB220001, Fondecyt Regular grant No. 1231172, Subvención a la Instalación en la Academia grant No. SA77210018. Also, the financial support from Vicerrectoría de Investigación, Innovación y Creación, USACH: JUV\_INVESTIGADORA\_DICYT\_USA21991 Grant No. 042431AA\_JUVI.

\* F. Albarrán-Arriagada [francisco.albarran@usach.cl](mailto:francisco.albarran@usach.cl)

- [1] F. Arute, K. Arya, R. Babbush, D. Bacon, J. C. Bardin, R. Barends, R. Biswas, S. Boixo, F. G. S. L. Brandao, D. A. Buell, B. Burkett, Y. Chen, Z. Chen, B. Chiaro, R. Collins, W. Courtney, A. Dunsworth, E. Farhi, B. Foxen, A. Fowler, C. Gidney, M. Giustina, R. Graff, K. Guerin, S. Habegger, M. P. Harrigan, M. J. Hartmann, A. Ho, M. Hoffmann, T. Huang, T. S. Humble, S. V. Isakov, E. Jeffrey, Z. Jiang, D. Kafri, K. Kechedzhi, J. Kelly, P. V. Klimov, S. Knysh, A. Korotkov, F. Kostritsa, D. Landhuis, M. Lindmark, E. Lucero, D. Lyakh, S. Mandrà, J. R. McClean, M. McEwen, A. Megrant, X. Mi, K. Michielsen, M. Mohseni, J. Mutus, O. Naaman, M. Neeley, C. Neill, M. Yuezhen Niu, E. Ostby, A. Petukhov, J. C. Platt, C. Quintana, E. G. Rieffel, P. Roushan, N. C. Rubin, D. Sank, K. J. Satzinger, V. Smelyanskiy, K. J. Sung, M. D. Trevithick, A. Vainsencher, B. Villalonga, T. White, Z. J. Yao, P. Yeh, A. Zalcman, H. Neven and J. M. Martinis. Quantum supremacy using a programmable superconducting processor. *Nature* **574**, 505 (2019).
- [2] H-S. Zhong, Y-H Deng, J. Qin, H. Wang, M-Ch. Chen, L-Ch. Peng, Y-H. Luo, D. Wu, S-Q Gong, H. Su, Y. Hu, P. Hu, X-Y. Yang, W-J Zhang, H. Li, Y. Li, X. Jiang, L. Gan, G. Yang, L. You, Z. Wang, L. Li, N-L Liu, J. J. Renema, C-Y. Lu, and J-W Pan, Phase-programmable gaussian boson sampling using stimulated squeezed light, *Phys. Rev. Lett.* **127**, 180502 (2021).



- [3] Y. Wu, W.-S. Bao, S. Cao, F. Chen, M.-C. Chen, X. Chen, T.-H. Chung, H. Deng, Y. Du, D. Fan, M. Gong, C. Guo, C. Guo, S. Guo, L. Han, L. Hong, H.-L. Huang, Y.-H. Huo, L. Li, N. Li, S. Li, Y. Li, F. Liang, C. Lin, J. Lin, H. Qian, D. Qiao, H. Rong, H. Su, L. Sun, L. Wang, S. Wang, D. Wu, Y. Xu, K. Yan, W. Yang, Y. Yang, Y. Ye, J. Yin, C. Ying, J. Yu, C. Zha, C. Zhang, H. Zhang, K. Zhang, Y. Zhang, H. Zhao, Y. Zhao, L. Zhou, Q. Zhu, C.-Y. Lu, C.-Z. Peng, X. Zhu, and J.-W. Pan, Strong Quantum Computational Advantage Using a Superconducting Quantum Processor, *Phys. Rev. Lett.* **127**, 180501 (2021).
- [4] L. Madsen, F. Laudenbach, M. F. Askarani, F. Rortais, T. Vincent, J. F. F. Bulmer, F. M. Miatto, L. Neuhaus, L. G. Helt, M. J. Collins, A. E. Lita, T. Gerrits, S. Woo Nam, V. D. Vaidya, M. Menotti, I. Dhand, Z. Vernon, N. Quesada and J. Lavoie. Quantum computational advantage with a programmable photonic processor, *Nature* **606**, 75 (2022).
- [5] Y. Kim, A. Eddins, S. Anand, K. X. Wei, E. van den Berg, S. Rosenblatt, H. Nayfeh, Y. Wu, M. Zaletel, K. Temme and A. Kandala. Evidence for the utility of quantum computing before fault tolerance, *Nature* **618**, 500 (2023).
- [6] P. J. J. O'Malley, R. Babbush, I. D. Kivlichan, J. Romero, J. R. McClean, J. R. R. Barends, J. Kelly, P. Roushan, A. Tranter, N. Ding, B. Campbell, Y. Chen, Z. Chen, B. Chiaro, A. Dunsworth, A. G. Fowler, E. Jeffrey, E. Lucero, A. Megrant, J. Y. Mutus, M. Neeley, C. Neill, C. Quintana, D. Sank, A. Vainsencher, J. Wenner, T. C. White, P. V. Coveney, P. J. Love, H. Neven, A. Aspuru-Guzik, and J. M. Martinis, Scalable quantum simulation of molecular energies, *Phys. Rev. X* **6**, 031007 (2016).
- [7] J. Biamonte, N. P. P. Wittek, P. Rebentrost, N. Wiebe, and S. Lloyd, Quantum machine learning, *Nature* **549**, 195–202 (2017).
- [8] E. Farhi, J. Goldstone, and S. Gutmann, A quantum approximate optimization algorithm, *arXiv:1411.4028* (2014).
- [9] S. Lloyd, Universal quantum simulators, *Science* **273**, 1073 (1996).
- [10] D. P. DiVincenzo, The physical implementation of quantum computation, *Fortschr. Phys.* **48**, 771 (2000).
- [11] Y. Nakamura, Y. A. Pashkin, and J. S. Tsai, Coherent control of macroscopic quantum states in a single-cooper-pair box, *Nature* **398**, 786 (1999).
- [12] J. I. Cirac and P. Zoller, Quantum computations with cold trapped ions, *Phys. Rev. Lett.* **74**, 4091 (1995).
- [13] E. Knill, R. Laflamme, and G. J. Milburn, A scheme for efficient quantum computation with linear optics, *Nature* **409**, 46(2001)
- [14] J. Preskill, Quantum Computing in the NISQ era and beyond, *Quantum* **2**, 79 (2018)
- [15] K. Bharti, A. Cervera-Lierta, T. H. Kyaw, T. Haug, S. Alperin-Lea, A. Anand, M. Degroote, H. Heimonen, J. S. Kottmann, T. Menke, W.-K. Mok, S. Sim, L.-C. Kwek, and A. Aspuru-Guzik, Noisy intermediate-scale quantum algorithms, *Rev. Mod. Phys.* **94**, 015004 (2022)
- [16] E. Farhi, J. Goldstone, S. Gutmann, J. Lapan, A. Lundgren, and D. Preda, A quantum adiabatic evolution algorithm applied to random instances of an np-complete problem, *Science* **292**, 472 (2001).
- [17] R. Barends, A. Shabani, L. Lamata, J. Kelly, A. Mezzacapo, U. Las Heras, R. Babbush, A. G. Fowler, B. Campbell, Yu Chen, Z. Chen, B. Chiaro, A. Dunsworth, E. Jeffrey, E. Lucero, A. Megrant, J. Y. Mutus, M. Neeley, C. Neill, P. J. J. O'Malley, C. Quintana, P. Roushan, D. Sank, A. Vainsencher, J. Wenner, T. C. White, E. Solano, H. Neven and J. M. Martinis, Digitized adiabatic quantum computing with a superconducting circuit, *Nature* **534**, 222 (2016).
- [18] D. Aharonov, W. van Dam, J. Kempe, Z. Landau, S. Lloyd, and O. Regev, Adiabatic quantum computation is equivalent to standard quantum computation, *45th Annual IEEE Symposium on Foundations of Computer Science*, 42 (2004).
- [19] A. Mizel, D. A. Lidar, and M. Mitchell, Simple Proof of Equivalence between Adiabatic Quantum Computation and the Circuit Model, *Phys. Rev. Lett.* **99**, 070502 (2007).
- [20] D. Guery-Odelin, A. Ruschhaupt, A. Kiely, E. Torrontegui, S. Martínez-Garaot, and J. G. Muga, Shortcuts to adiabaticity: Concepts, methods, and applications, *Rev. Mod. Phys.* **91**, 045001 (2019).
- [21] M. Demirplak and S. A. Rice, Adiabatic population transfer with control fields, *J. Phys. Chem. A* **107**, 9937(2003).
- [22] M. Demirplak and S. A. Rice, Assisted adiabatic passage revisited, *J. Phys. Chem. A* **109**, 6838 (2005).
- [23] M. V. Berry, Transitionless quantum driving, *J. Phys. A* **42**, 365303 (2009).
- [24] D. Sels and A. Polkovnikov, Minimizing irreversible losses in quantum systems by local counterdiabatic driving, *PNAS* **114**, E3909 (2017).
- [25] T. Hatomura and K. Takahashi, Controlling and exploring quantum systems by algebraic expression of adiabatic gauge potential. *Phys. Rev. A* **103**, 012220 (2021).
- [26] P. W. Claeys, M. Pandey, D. Sels, and A. Polkovnikov, Floquet engineering counterdiabatic protocols in quantum many-body systems. *Phys. Rev. Lett.* **123**, 090602 (2019).
- [27] S. Morawetz and A. Polkovnikov, Efficient paths for local counterdiabatic driving, *Phys. Rev. B* **110**, 024304 (2024).
- [28] I. Čepaitė, A. Polkovnikov, A. J. Daley, and C. W. Duncan, Counterdiabatic optimized local driving, *PRX Quantum* **4**, 010312 (2023).
- [29] N. N. Hegade, K. Paul, Y. Ding, M. Sanz, F. Albarrán-Arriagada, E. Solano, and X. Chen, Shortcuts to Adiabaticity in Digitized Adiabatic Quantum Computing, *Phys. Rev. Appl.* **15**, 024038 (2021).
- [30] J. Wurtz and P. J. Love. Counterdiabaticity and the quantum approximate optimization algorithm, *Quantum* **6**, 635 (2022).
- [31] P. Chandarana, N. N. Hegade, K. Paul, F. Albarrán-Arriagada, E. Solano, A. del Campo, and X. Chen, Digitized counterdiabatic quantum approximate optimization algorithm, *Phys. Rev. Res.* **4**, 013141 (2022).
- [32] N. N. Hegade, K. Paul, F. Albarrán-Arriagada, X. Chen, and E. Solano, Digitized adiabatic quantum factorization, *Phys. Rev. A* **104**, L050403 (2021).
- [33] P. Chandarana, N. N. Hegade, I. Montalban, E. Solano, and X. Chen, Digitized counterdiabatic quantum algorithm for protein folding, *Phys. Rev. Appl.* **20**, 014024 (2023).
- [34] N. N. Hegade, P. Chandarana, K. Paul, X. Chen, F. Albarrán-Arriagada, and E. Solano, Portfolio optimization with digitized counterdiabatic quantum algorithms, *Phys. Rev. Res.* **4**, 043204 (2022).
- [35] M. Luo and X. Wang. Universal quantum computation with qudits, *Sci. China Phys. Mech. Astron.* **57**, 1712 (2014).
- [36] Y. Wang, Z. Hu, B. C. Sanders, and S. Kais, Qudits and high-dimensional quantum computing, *Front. Phys.* **8**, 589504 (2020).
- [37] S. Paesani, J. F. F. Bulmer, A. E. Jones, R. Santagati, and A. Laing, Scheme for universal high-dimensional quantum computation with linear optics, *Phys. Rev. Lett.* **126**, 230504 (2021).
- [38] A. Cervera-Lierta, M. Krenn, A. Aspuru-Guzik, and A. Galda, Experimental high-dimensional greenberger-horne-zeilinger entanglement with superconducting transmon qutrits, *Phys. Rev. Appl.* **17**, 024062 (2022).

- [39] M. Ringbauer, M. Meth, L. Postler, P. Schindler and T. Monz, A universal qudit quantum processor with trapped ions, *Nat. Phys.* **18**, 1053 (2022).
- [40] Y. Wang, S. Ru, F. Wang, P. Zhang, and F. Li, Experimental demonstration of efficient high-dimensional quantum gates with orbital angular momentum, *Quantum Sci. Technol.* **7**, 015016 (2021).
- [41] N. Goss, A. Morvan, B. Marinelli, B. K. Mitchell, L. B. Nguyen, R. K. Naik, L. Chen, C. Jünger, J. M. Kreikebaum, D. I. Santiago, J. J. Wallman and I. Siddiqi, High-fidelity qutrit entangling gates for superconducting circuits, *Nat Commun* **13**, 7481 (2022).
- [42] K. Luo, W. Huang, Z. Tao, L. Zhang, Y. Zhou, J. Chu, W. Liu, B. Wang, J. Cui, S. Liu, F. Yan, M.-H. Yung, Y. Chen, T. Yan, and D. Yu, Experimental realization of two qutrits gate with tunable coupling in superconducting circuits, *Phys. Rev. Lett.* **130**, 030603 (2023).
- [43] P. Hrmo, B. Wilhelm, L. Gerster, M. W. van Mourik, M. Huber, R. Blatt, P. Schindler, T. Monz and M. Ringbauer, Native qudit entanglement in a trapped ion quantum processor, *Nat Commun* **14**, 2242 (2023).
- [44] H. Markowitz, Portfolio selection, *J. Finance* **7**, 77 (1952).
- [45] Q. Xie, K. Seki, and S. Yunoki, Variational counterdiabatic driving of the hubbard model for ground-state preparation, *Phys. Rev. B* **106**, 155153 (2022).
- [46] A. B. Kilmov, R. Guzmán, J. C. Retamal, and C. Saavedra, Qutrit quantum computer with trapped ions, *Phys. Rev. A* **67**, 062313 (2003).
- [47] M. A. Nielsen and I. Chuang, *Quantum Computation and Quantum Information* (Cambridge University Press, 2000).
- [48] <https://github.com/ranaroussi/yfinance>

## APPENDIX A: QUBITS FORMULATION

Next we provide the qubit-based Hamiltonians used to compare with qutrit codification. For all the case the initial Hamiltonian is given by the usual one

$$H_I = \omega_0 \sum_j X_j^{(2)}, \quad (40)$$

where the subindex  $j$  refers to the  $j$ th qubit and the matrix  $X^{(2)}$  is given by:

$$X^{(2)} = \begin{pmatrix} 0 & 1 \\ 1 & 0 \end{pmatrix}, \quad (41)$$

therefore, the initial state is also a uniform superposition states of computational basis.

For codify a trinary variable with values  $-1, 0, 1$  we need use two qubits in a way that the combination only allows the values of trinary variable. Therefore, for the final Hamiltonian we use exact the same expression for Multiway number partitioning and Max 3-cut but we replace the qutrit operator  $Z$  for the following qubits operators:

$$Z_i \rightarrow \frac{Z_{2i-1}^{(2)} + Z_{2i}^{(2)}}{2}, \quad (42)$$

where the matrix  $Z^{(2)}$  is given by:

$$Z^{(2)} = \begin{pmatrix} 1 & 0 \\ 0 & -1 \end{pmatrix}. \quad (43)$$

Therefore, this combination of two qubits guarantees that the possible values are  $-1, 0, 1$ . For multi-way number partitioning, the final Hamiltonian with qubits formulation is:

$$\begin{aligned} H_F = & \frac{1}{16} \sum_{j,k} \left( 9(I + Z_{2j-1}^{(2)} Z_{2j}^{(2)})(I + Z_{2k-1}^{(2)} Z_{2k}^{(2)}) \right. \\ & - 6(I + Z_{2j-1}^{(2)} Z_{2j}^{(2)})(Z_{2k-1}^{(2)} + Z_{2k}^{(2)}) - 24(I + Z_{2j-1}^{(2)} Z_{2j}^{(2)}) \\ & + 8(Z_{2j-1}^{(2)} + Z_{2j}^{(2)}) + 5(Z_{2j-1}^{(2)} + Z_{2j}^{(2)})(Z_{2k-1}^{(2)} + Z_{2k}^{(2)}) \\ & \left. + 16 \right) s_j s_k, \end{aligned} \quad (44)$$

where we use the replace of  $G_j$  by:

$$G_j \rightarrow \frac{I + Z_{2i-1}^{(2)} Z_{2i}^{(2)}}{2}, \quad (45)$$

obtained by squaring the equation 42. In the same way, the final Hamiltonian for max 3-cut with qubits formulation is:

$$\begin{aligned} H_F = & \frac{1}{4} \sum_{(j,k) \in E} \left[ (1 + \alpha)(I + Z_{2j-1}^{(2)} Z_{2j}^{(2)})(I + Z_{2k-1}^{(2)} Z_{2k}^{(2)}) \right. \\ & + (Z_{2j-1}^{(2)} + Z_{2j}^{(2)})(Z_{2k-1}^{(2)} + Z_{2k}^{(2)}) \\ & \left. - 2\alpha(2 + Z_{2j-1}^{(2)} Z_{2j}^{(2)} + Z_{2k-1}^{(2)} Z_{2k}^{(2)}) \right], \end{aligned} \quad (46)$$

For portfolio optimization we have the label  $u$  for qutrit operator  $Q$ , necessary for correct assignation of position for codify the integer number  $p_j$  in trinary representation. In addition, the possible values are  $0, 1, 2$ , so we need a different combination of two qubits. We use the following change of qutrit operator  $Q$  for qubits:

$$Q_u \rightarrow Q_v^{(2)} + 2Q_{v+1}^{(2)}, \quad (47)$$

where the matrix  $Q^{(2)}$  is given by:

$$Q^{(2)} = \begin{pmatrix} 1 & 0 \\ 0 & 0 \end{pmatrix}, \quad (48)$$

and the label  $v$  is a short expression of  $v(j, k) = (j - 1)2g + k$ . In this case, the replace of qutrit operator  $Q$  for qubits operators of equation 47 need a penalization when  $Q_v^{(2)}$  and  $Q_{v+1}^{(2)}$  are equal 1. We include the following term to  $H_F$ :

$$P = \theta_4 \sum_j Q_{2j}^{(2)} Q_{2j-1}^{(2)}, \quad (49)$$

where  $\theta_4$  is a Lagrange multiplier that ponderate the penalization when both qubits are equal 1. Therefore the final Hamiltonian of portfolio optimization with qubit formulation is:

$$\begin{aligned} H_F = & \sum_{j=1}^n \sum_{k=1}^g \alpha_{jk} (Q_v^{(2)} + 2Q_{v+1}^{(2)}) \\ & + \sum_{j,j'=1}^n \sum_{k,k'=1}^g \beta_{jj'}^{kk'} (Q_v^{(2)} + 2Q_{v+1}^{(2)}) (Q_{v'}^{(2)} + 2Q_{v'+1}^{(2)}) + \theta_3 b^2 \\ & + \theta_4 \sum_{j=1}^{ng} Q_{2j}^{(2)} Q_{2j-1}^{(2)}. \end{aligned} \quad (50)$$